ISSN (Online): 2455-3662
EPRA International Journal of Multidisciplinary Research (IJMR) - Peer Reviewed Journal
Volume: 9| Issue: 10| October 2023|| Journal DOI: 10.36713/epra2013 || SJIF Impact Factor 2023: 8.224 || ISI Value: 1.188

ELECTROMAGNETIC FIELD IMPROVEMENT IN PERMANENT MAGNET SYNCHRONOUS MOTOR

Jonathan Emmanuel Mangeleka[a*], Donghai Hu[a]
[a]*School of Automotive and Traffic Engineering, Jiangsu University, Zhenjiang 212013, China*
[*]*Correspondence to: Jonathan Emmanuel Mangeleka*

Article DOI: https://doi.org/10.36713/epra14697
DOI No: 10.36713/epra14697

ABSTRACT
Permanent magnet synchronous motors (PMSMs) have recently been popular and widely used for electrical vehicle developments in the automobile industry to replace internal combustion engines due to their ability to perform at higher efficiency. This paper uses the PMSM in fuel cell vehicle electric air compressors. To ensure that the PMSM performs at higher efficiency, some field performance, such as electromagnetic field, must be improved. In this paper, a comparison between the electromagnetic forces components in the presence of current harmonic. The data indicates that the amplitude of electromagnetic forces for both radial and tangential components are not the same, particularly in lower orders. However, radial forces' contribution is greater than tangential forces. A structural optimization method reduces the radial electromagnetic (RE) forces to improve PMSM's efficiency. The optimization method involves changes in the PMSM's design values and improving the electromagnetic field performance. The RE forces found to dominate the tangential electromagnetic (TE) forces, and it's amplitudes corresponding to 2,4 and 6-order are minimized by 31.1%, 28.5%, and 15.9%, respectively.

KEYWORDS: ***Tangential electromagnetic forces; radial electromagnetic forces; permanent magnet synchronous motor; optimization***

1. INTRODUCTION

PMSMs deliver a high-power density, remarkable efficiency, and customizable speed, which is among the reasons they are often used in electric vehicles. In a new energy vehicle, the motor is the core component of the power system and the main source of excitation for electromagnetic vibration. Due to its significant role, it has also gained much attention in electromagnetic performance research.

With electromagnetic excitation comes electromagnetic problems involving the studies on performance features of PMSM to analyze the distribution characteristics of electromagnetic forces from the excitation field and to minimize the electromagnetic forces based on the resulting phenomenon of distribution [2]. The electromagnetic torque produced from the tangential electromagnetic force component causes torque ripple and cogging torque, which minimally affects electromagnetic vibration and noise. In contrast, radial electromagnetic force is the primary source [3,4]. Effective studies such as stator and structure optimization [5], pole-arc coefficient [6], slots design [7], improving the rotor structure [8], and decrease of harmonics of the air gap flux density [9] can result in improvement of electromagnetic filed performances. As for rotor skewing, it also weakens cogging torque and torque ripple to improve electromagnetic field characteristics [10,11]. However, some recent rotor designs are smooth, such as the PMSM used in this paper. Since many factors cause the cogging torque, its minimum quantity does not always ensure low torque ripple [12], and no matter what measures are taken, it can only be restrained to a certain extent for the slotted permanent magnet motor, and it is difficult to eliminate it completely [13]. The output torque is important not to be affected during the optimization of motor electromagnetic performance, Wang et al. [10] did torque ripple reduction by rotor slotting, which optimized motor's NVH performance but affected the output torque. This also applies to the motor characteristics by Mendizabal et al. [14]. Jung et al. [15] used the equivalent magnetization current method to evaluate the electromagnetic excitation force acting on the motor stator system. Initially, on loading form of the electromagnetic force, the electromagnetic force is applied to the stator tooth surface in the form of a centered force. The method is effective, but the study influence of force components is necessary for optimization purposes.

The paper will involve a multi-physics coupling method to predict the electromagnetic performance of PMSM. A model is presented to calculate the motor's electromagnetic forces, which are verified by the theoretical formulations. Based on the results, an

ISSN (Online): 2455-3662
EPRA International Journal of Multidisciplinary Research (IJMR) - Peer Reviewed Journal
Volume: 9| Issue: 10| October 2023|| Journal DOI: 10.36713/epra2013 || SJIF Impact Factor 2023: 8.224 || ISI Value: 1.188

optimization method that involves changes in the PMSM's design values is adopted to improve the electromagnetic field performance.

2. NUMERICAL EQUATIONS AND SIMULATION OF ELECTROMAGNETIC FIELD

The high-speed PMSM in this research is used as a driving machine for the fuel cell electric air compressor. It comprises a magnetic rotor, rotor shaft, stator core, front and rear end cover, housing, and stator windings.

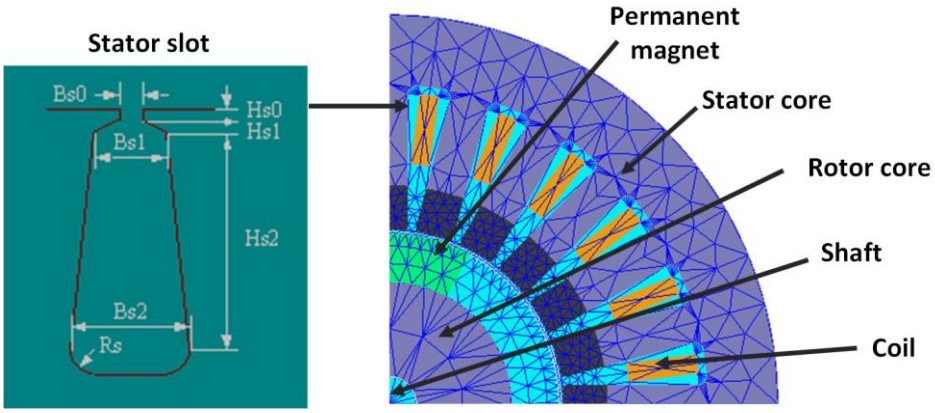

Fig. 1. SHSPMSM structure.

Table 1. Main parameters of PMSM

Parameter	Value	Parameter	Value
Rated power	20kw	Stator diameter	71mm
Rated speed	60krpm	Rotor diameter	37.6mm
Rated voltage	370V	Air-gap length	0.45mm
Slots/pole	24/2	Pole-arc coefficient	0.55

2.2 Numerical Equations

Considering that there is no slotting on the rotor structure surface SHSPMSM, the air gap magnetic conductance $\lambda(\theta, t)$ expression is:

$$\lambda(\theta,t) = \Lambda_0 + \sum_{k=1}^{\infty} \Lambda_k \cos kZ_1\theta \tag{1}$$

where, Λ_0 is the average magnetic permeability amplitude Λ_k is k-th harmonic magnetic permeability amplitude, k is harmonic order, θ is the positioning angle at the circumference, and Z_1 is the slot numbers.

In PMSM, the magnetic flux density calculates the electromagnetic forces acting on the stator teeth's outer surface. The electromagnetic force is calculated and then split into tangential and radial components from the stator teeth's surface. The air-gap magnetic field harmonics and the electromagnetic forces and relationship are described from the Maxwell stress tensor method [16], where both electromagnetic forces components of tangential and radial are described below:

$$\begin{cases} f_r = \dfrac{B_r(\theta,t)^2 - B_t(\theta,t)^2}{2\mu_0} \approx \dfrac{B_r(\theta,t)^2}{2\mu_0} \\ f_t = \dfrac{B_r(\theta,t)B_t(\theta,t)}{\mu_0} \end{cases} \tag{2}$$

ISSN (Online): 2455-3662
EPRA International Journal of Multidisciplinary Research (IJMR) - Peer Reviewed Journal
Volume: 9| Issue: 10| October 2023|| Journal DOI: 10.36713/epra2013 || SJIF Impact Factor 2023: 8.224 || ISI Value: 1.188

where, $B_r(\theta,t)$ and $B_t(\theta,t)$, are radial and tangential air-gap magnetic flux density components, respectively as stated by Equation (3).

Defining f_u and f_v as:

$$\begin{cases} f_\mu = \sum_\mu F_\mu \cos(\mu \frac{\omega_1}{p} t - \mu\theta), \mu = (2r+1)p, r = 0,1,2,3.... \\ f_\nu = \sum_\nu F_\nu \cos(\omega_1 t - \nu\theta + \psi), \nu = (6k+1)p, k = \pm1, \pm2, \pm3... \end{cases} \quad (3)$$

where, μ is the harmonic spatial modulus of a permanent magnet (PM), p is the pole pairs number, F_μ is the amplitude of the magnetomotive harmonic force of the PM, ω_1 is the current angular velocity, and f_1 is the current frequency.

Substitute Equations (3) into $B_r(\theta,t)$. The radial air-gap magnetic flux density components further expanded as:

$$\begin{aligned} B_r(\theta,t) &= \left[\sum_{\mu/p} F_\mu \cos(\mu \frac{\omega_1}{p} t - \mu\theta) + \sum_\nu F_\nu \cos(\omega_1 t - \nu\theta + \psi)\right]\left[\Lambda_0 + \sum_{k=1}^{\infty} \Lambda_k \cos kZ_1\theta\right] \\ &= \left[\begin{array}{l} \sum_\mu \Lambda_0 F_\mu \cos(\mu \frac{\omega_1}{p} t - \mu\theta) + \sum_\nu \Lambda_0 F_\nu \cos(\omega_1 t - \nu\theta + \varphi) + \\ \sum_{k=1}^{\infty}\sum_\mu \Lambda_k F_\mu \cos kZ_1\theta \cos(\mu \frac{\omega_1}{p} t - \mu\theta) + \\ \left\{\sum_{k=1}^{\infty} \sum_\nu \Lambda_k F_\nu \cos kZ_1\theta \cos(\omega_1 t - \nu\theta + \varphi)\right\} \end{array}\right] \end{aligned} \quad (4)$$

The final equation is obtained from Equation (2) and expressed as:

$$f_r(\theta,t) = \frac{1}{2\mu_0}\left[\sum_{\mu/p} \Lambda_0 F_\mu \cos(\mu \frac{\omega_1}{p} t - \mu\theta) + \sum_{\nu/p} \Lambda_0 F_\nu \cos(\omega_1 t - \nu\theta + \varphi)\right]^2 \quad (5)$$

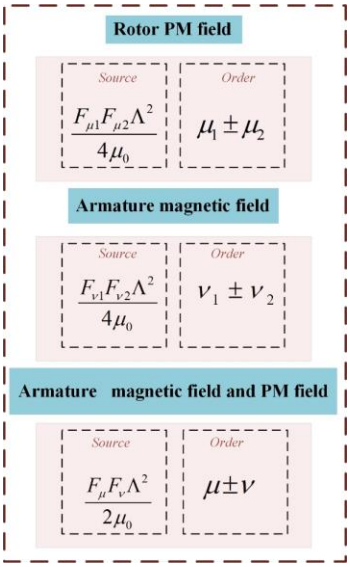

Figure 2: Electromagnetic features of the motor

ISSN (Online): 2455-3662
EPRA International Journal of Multidisciplinary Research (IJMR) - Peer Reviewed Journal
Volume: 9| Issue: 10| October 2023|| Journal DOI: 10.36713/epra2013 || SJIF Impact Factor 2023: 8.224 || ISI Value: 1.188

The self-action on the magnetic field of the rotor causing the RE force. The order of this RE force is expressed as:

$$\gamma = \mu_i \pm \mu_j = 2(r_i + r_j + 1)p(or)2(r_i - r_j)p \qquad (6)$$

where, μ_i and μ_j represent the *i*-th and *j*-th harmonics of the magnetic density of the rotor poles, respectively. The electromagnetic force frequency is expressed as:

$$f = 2(r_i + r_j + 1)f_1(or)2(r_i - r_j)f_1 \qquad (7)$$

where, f_1 is the frequency of the current. It is customary to take the rotational frequency as the base value for rotating machinery. If f_0 is the frequency of the motor rotor rotation and $pf_0 = f_1$ while the RE force frequency generated by the self-action of the stator armature magnetic field can be rewritten as:

$$f = 2(r_i + r_j + 1)pf_0(or)2(r_i - r_j)pf_0 \qquad (8)$$

In this paper, the PMSM the pole number *p* is 1. So, the order of RE force generated by the rotor magnetic pole is expressed as: $\gamma = \mu_i \pm \mu_j = 2(r_i + r_j + 1)or\,2(r_i - r_j)$ and the frequency of RE force as: $f = 2(r_i + r_j + 1)f_0 or 2(r_i - r_j)f_0$.

The RE force caused by the self-action of the stator armature magnetic field is expressed as:

$$\gamma = \nu_i \pm \nu_j = 2(3k_i + 3k_j + 1)(or)2(3k_i - 3k_j) \qquad (9)$$

where, ν_i and ν_j represent the *i*-th and *j*-th harmonics of the armature magnetic field density, respectively. The frequency of the RE force is:

$$f = 2f_1 = 2pf_0 \qquad (9)$$

Therefore, the order of RE force after the armature is energized and expressed as: $\gamma = \nu_i \pm \nu_j = 2(3k_i + 3k_j + 1)$. The frequency of RE force is: $f = 2f_0$

The RE force generated by the joint action of the armature magnetic field and rotor PM magnetic field is expressed as:

$$\gamma = \mu_i + \nu_j = 2(r_i + 3k_j + 1)p(or)2(r_i - 3k_j)p \qquad (10)$$

where, μ_i and μ_j represent the *i*-th harmonic of the rotor magnetic pole magnetic density and the *j*-th harmonic of the armature magnetic field magnetic density, respectively. The frequency of the RE force is:

$$f = 2(r_i + 1)pf_0(or)2r_i pf_0 \qquad (11)$$

Therefore, the spatial modulus of the RE force of the joint action between the rotor magnetic pole and armature reaction is expressed as: $\gamma = \mu_i + \nu_j = 2(r_i + 3k_j + 1)or\,2(r_i - 3k_j)$. The frequency of RE force is: $f = 2(r_i + 1)f_0 or 2r_i f_0$. Generalization of the electromagnetic force sources from Figure 3 concludes that their characteristic order is $\gamma = 2pn$. N is a natural number, and 2*p* is the number of magnetic poles.

2.1 Electromagnetic field numerical simulation

A finite element model of the PMSM in ANSYS software is created for simulation and calculations based on its specified structural parameters. The flux density and magnetic force distribution contours in the PMSM under load are depicted in Figure 3.

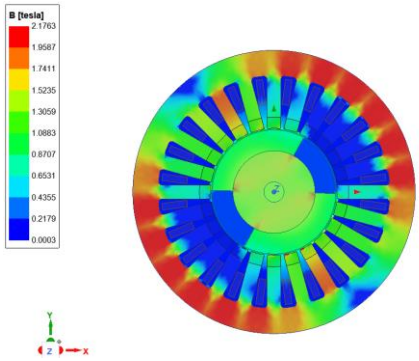

Fig 3. Flux Density Distribution

A transient field solver calculates the motor's air gap magnetic density and RE force at the rated speed. In ANSYS Maxwell software, in order to solve the distribution of motor air gap magnetic density, a fixed time during motor operation is taken and calculated along the arc path of the air gap center. A custom calculation script is imported since the Maxwell 2D module does not directly solve tangential and radial magnetic densities. It is necessary to use Equations (12) and (13) in the Maxwell 2D analysis module and use the air gap magnetic flux density of the x-axis and y-axis components to solve the tangential and radial air gap magnetic flux density.

ISSN (Online): 2455-3662
EPRA International Journal of Multidisciplinary Research (IJMR) - Peer Reviewed Journal
Volume: 9| Issue: 10| October 2023|| Journal DOI: 10.36713/epra2013 || SJIF Impact Factor 2023: 8.224 || ISI Value: 1.188

$$B_r = B_x \cos\theta + B_y \sin\theta \quad (12)$$

$$B_t = B_x \sin\theta + B_y \cos\theta \quad (13)$$

Where B_r and B_t are -radial and tangential air gap magnetic flux density, respectively. B_y and B_x - the y-axis and x-axis components of air gap magnetic flux density, respectively. θ is the angle between the line connecting the midpoint of the air gap and the origin and the x-axis. A created circular path near the inner wall of the stator core in the air gap between the stator and rotor solves the tangential and radial air gap magnetic flux densities. Electromagnetic excitation information is obtained through circuit models or by collecting measured phase currents. Then, the electromagnetic finite element model calculates the magnetic field air gap and electromagnetic forces of the PMSM.

In order to extract electromagnetic forces amplitude value, the finite element (FE) model in Figure 1 is utilized to immediately determine the PMSM's air-gap magnetic field components of at the rated speed. A script is applied to determine the order and amplitude of electromagnetic forces. The RE force is used as an objective function for optimal design since its amplitude dominates the TE force.

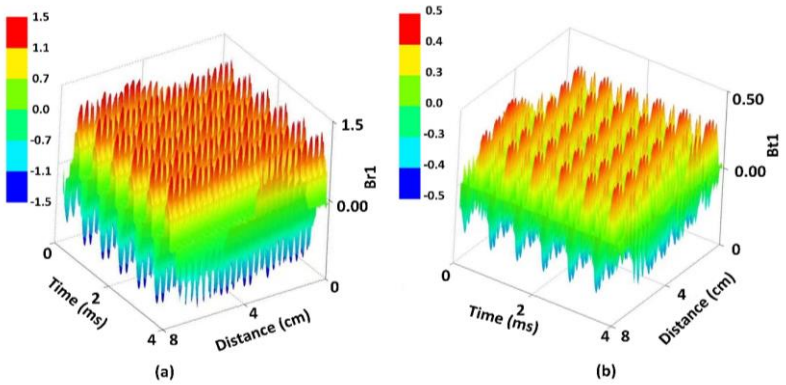

Fig 4. 3D distribution of the electromagnetic force components of the SHSPMSM; (a): Radial force (b): Tangential force

In Figure 4, magnetic density distribution in RE component appears with higher amplitudes than the TE components. The waveforms of electromagnetic forces in time-domain data are changed into frequency-domain data by imposing Fast Fourier Transform (FFT) decomposition. The order characteristics of radial and TE forces for the SHSPMSM are shown in Figure. 5.

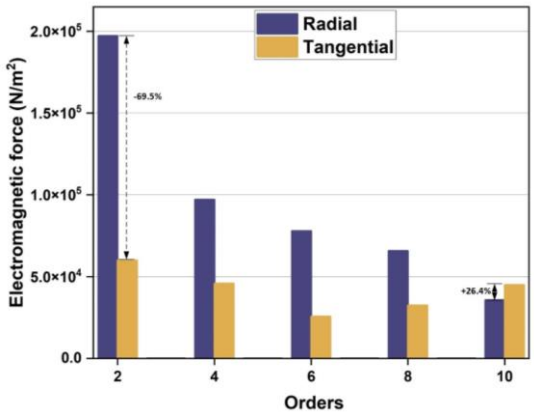

Fig. 4. Order characteristics of RE and TE forces.

In low-order harmonics, the RE forces amplitudes of the PMSM concentrate in 2, 4, 6, 8, and 10th order. For RE force, the peak appears on 2-order, which is 69.5% larger than the same TE force order. While, for TE force, the peak appears on order of 10, which is 26.4% larger than the RE force amplitude. Therefore, the radial forces dominate the tangential forces. The electromagnetic field results provide empirical support that the characteristic frequencies of the RE forces of the SHSPMSM are even multiple of the fundamental frequency, $2nf_o$ (n=1, 2….). The simulation results in Fig. 4 on amplitudes of harmonic orders are on good terms with the electromagnetic theory of the PMSM.

ISSN (Online): 2455-3662
EPRA International Journal of Multidisciplinary Research (IJMR) - Peer Reviewed Journal
Volume: 9| Issue: 10| October 2023|| Journal DOI: 10.36713/epra2013 || SJIF Impact Factor 2023: 8.224 || ISI Value: 1.188

3. IMPROVEMENT RESULTS AND DISCUSSION

To improve electromagnetic performance of the motor, a multi-objective optimization method is used, and all design requirements are met. The traditional optimization methods only consider a single aim, which can influence the general results, but Kennedy and Eberhart [31] proposed particle swarm optimization (PSO) to be applied to problems with multiple problems. The air gap length and the stator slot design parts of the PMSM are the design variables, while output electromagnetic torque and radial electromagnetic force are objective functions. The mathematical function for the motor is expressed as follows:

$$\begin{cases} Max_{x\in V} T_j(X) \\ Min_{x\in V} f_{pr}(X) \\ V = \{\{X|x_1 \in [0.3-0.6]\},\{X|x_2 \in [0.5-1]\},\{X|x_3 \in [0.4-1]\}, \\ \{X|x_4 \in [0.5-1.5]\},\{X|x_5 \in [5-20]\}\} \end{cases} \quad (3)$$

After the calculations, the air gap length before and after optimization is shown in Table 2. The electromagnetic torque increases, and the maximum amplitude of radial electromagnetic forces reduces from their initial design values. The electromagnetic performance of the motor is simulated based on the obtained new design values, while the working conditions of the PMSM are kept the same. Table 1 shows the results of the PMSM before and after improvement.

Table 1. Before and after structure improvement of the SHSPMSM

Parameter [mm]	Range	Before improvement	After improvement
Air gap length	0.3-0.6	0.45	0.56
H_{s0}	0.5-1	0.75	0.8
H_{s1}	0.4-1	0.73	0.81
B_{s0}	0.5-1.5	1	0.75
H_{s2}	5-20	12.7	15.12
R_s	1	1	1

The key to improving the electromagnetic performance of the PMSM is to weaken the respective orders of RE force amplitude. Before optimization, it's likely that the acoustic field can also be affected by electromagnetic field outcomes. As shown in Figure 5, the low-harmonic orders of RE force amplitude corresponding to 2*n*- order (*n*= 1, 2, and 3) are reduced by 31.1%, 28.5%, and 15.9%, respectively. The motor's efficiency also increases, as shown in Figure 6.

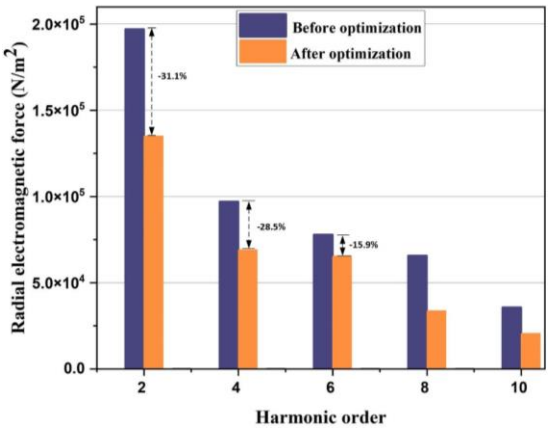

Fig. 5. Orders of RE force before and after improvement.

ISSN (Online): 2455-3662
EPRA International Journal of Multidisciplinary Research (IJMR) - Peer Reviewed Journal
Volume: 9| Issue: 10| October 2023|| Journal DOI: 10.36713/epra2013 || SJIF Impact Factor 2023: 8.224 || ISI Value: 1.188

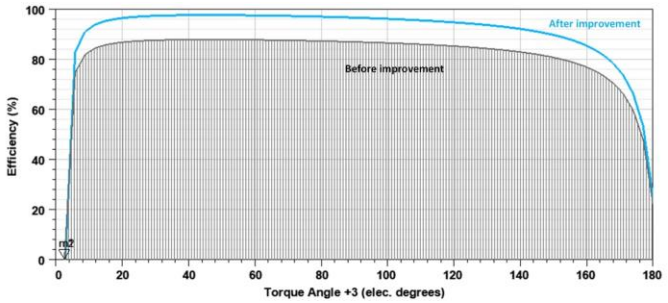

Fig. 6. PMSM efficiency before and after improvement.

4. CONCLUSION

Based on the numerical simulation of electromagnetic field results, the analysis provides an outlook for structure design optimization of the PMSM. The multi-objective optimization is used, and all the design needs are met. The following are the conclusions:

1. The RE forces amplitudes are predominantly in the low harmonic orders of the low-harmonic orders of radial electromagnetic force whose amplitudes correspond to 2*n*-order (*n*= 1, 2, and 3). For RE force, the peak appears on 2-order, which is 69.5% larger than the same TE force order. While, for TE force, the peak appears on order of 10, which is 26.4% larger than the RE force amplitude
2. The radial electromagnetic forces' amplitudes corresponding to 2, 4, and 6-order are minimized by 31.1%, 28.5%, and 15.9%, respectively.

REFERENCE

1. *W. Deng and S. Zuo. (2022), "Analysis of the Sideband Electromagnetic Noise in Permanent Magnet Synchronous Motors Generated by Rotor Position Error," in IEEE Transactions on Industrial Electronics, vol. 69, no. 5, p.p: 4460-4471*
2. *Dong. Q. C, Liu. X. T, Qi. H. Z, et al. (2019), "Analysis and evaluation of electromagnetic vibration and noise in permanent magnet synchronous motor with rotor Step skewing," Sci China Tech Sci, 62, p.p: 839–848*
3. *Lan, Hua & Zou, Jibin & Xu, Yongxiang & Zhao, Bo. (2017), "Analysis of Global and Local Force Harmonics and Their Effects on Vibration in Permanent Magnet Synchronous Machines, "IEEE Transactions on Energy Conversion. p.p: 1-1*
4. *Wang. S and Li. H.F. (2021), "Effects of Rotor Skewing on the vibration of Permanent Magnet Synchronous Motors with Elastic-Plastic Stator, "IEEE Transactions on Energy Conversion. p.p: 1-1.*
5. *Li X.H, Zhang L.F, Ying H.L, Huang S.R, and Zhang Q. (2020), "Study of Suppression of Vibration and Noise of PMSM for Electric Vehicles, "IET Electric Power Applications. Vol. 14*
6. *Liu, Feng & Wang, Xiuhe & Xing, Zezhi & Yu, Aiguo & Li, Changbin. (2021), "Reduction of cogging torque and electromagnetic vibration based on different combination of pole arc coefficient for interior permanent magnet synchronous machine, "CES Transactions on Electrical Machines and Systems. 5.p.p: 291-300.*
7. *Hu, Yaohua & Zhu, Shushu & Xu, Lilin & Jiang, Bin. (2021), "Reduction of Torque Ripple and Rotor Eddy Current Losses by Closed Slots Design in a High-speed PMSM for EHA Applications, "IEEE Transactions on Magnetics. p.p: 1-1*
8. *Wang, S., Li, H. (2020), "Reduction of Electromagnetic Vibration and Noise in Permanent Magnet Motor for EVs by Optimizing Design of Rotor Based on GPR-PSO Model, "Journal of Electrical Engineering & Technology. 15. p.p:1231-1243*
9. *Wang, Yongchao & Gao, Hui & Wang, Haiyang & Ma, Wenpeng. (2020), "NVH Optimization Analysis of Permanent Magnet Synchronous Motor by Rotor Slotting, "Vehicles. 2. p.p:287-303.*
10. *C. Peng, D. Wang, Z. Feng and B. Wang. (2022), "A New Segmented Rotor to Mitigate Torque Ripple and Electromagnetic Vibration of Interior Permanent Magnet Machine," in IEEE Transactions on Industrial Electronics, vol. 69, no. 2, p.p: 1367-1377*
11. *Wang, Xiaoyuan & Sun, Xibin & Gao, Peng. (2019), "A Study on the Effects of Rotor Step Skewing on the Vibration and Noise of a PMSM for Electric Vehicles, "IET Electric Power Applications*
12. *Fang, Haiyang & Li, Dawei & Qu, Ronghai & Yan, Peng. (2018), "Modulation Effect of Slotted Structure on Vibration Response in Electrical Machines, "IEEE Transactions on Industrial Electronics. p.p. 1-1.*
13. *Wenjie, Cheng & Cao, Guangdong & Zhikai, Deng & Xiao, Ling & Li, Ming. (2021), "Torque Comparison Between Slotless and Slotted Ultra-high Speed AFPM Motors Using Analytical Method, "IEEE Transactions on Magnetics. p.p: 1-1*
14. *Mendizabal, Mikel & McCloskey, Alex & Poza, Javi & Zárate, Sergio & Iriondo, Jaione & Irazu, Leire. (2021), "Optimum Slot and Pole Design for Vibration Reduction in Permanent Magnet Synchronous Motors, "Applied Sciences. 11. p.p: 4849.*
15. *Jung. J.-W, Kim. D.-J, Hong. J.-P, Lee. .G-H, and Jeon. S.-M. (2011) "Experimental verification and effects of step skewed rotor type IPMSM on vibration and noise," IEEE Trans Magn, vol. 47, no. 10, p.p: 3661–3664*
16. *Islam. M. S, Islam. R, and Sebastian. T. (2014), "Noise and vibration characteristics of permanent-magnet synchronous motors using electromagnetic and structural analyses," IEEE Trans Ind Appl, vol. 50, no. 5, p.p: 3214–3222*